

莱芜猪肌肉脂肪和皮下脂肪转录组分析

冯 卉, 刘天义, SALSABEEL Yousuf, 苗向阳*

(中国农业科学院 北京畜牧兽医研究所, 中国北京 100193)

摘要: 为探究莱芜猪中不同部位脂肪沉积产生差异的关键基因, 以180日龄体重相近的莱芜猪为实验对象, 鉴定肌肉脂肪(intramuscular fat, IMF)和皮下脂肪(subcutaneous fat, SCF)的mRNA表达谱, 对差异表达mRNA进行基因本体论(Gene Ontology, GO)与京都基因和基因组数据库(Kyoto Encyclopedia of Genes and Genomes, KEGG)功能富集分析, 构建平均表达量前300mRNA的蛋白质互作网络, 筛选关键调控mRNA, 并分析关键mRNA对应基因的序列和蛋白质结构, 探究基因表达水平、结构和功能的联系, 最后随机挑选6个mRNA进行实时荧光定量PCR(real-time fluorescence quantitative PCR, qRT-PCR)验证。筛选结果显示, 在IMF和SCF中共鉴定出1665个差异表达的mRNA, 其中888个上调, 777个下调。GO结果显示, 差异表达mRNA显著富集于信号通路调节的生物过程条目、生物膜组成的细胞组成条目和细胞代谢过程中酶活性调节的分子功能条目。KEGG富集结果显示, 差异表达mRNA主要参与脂肪细胞生成、脂代谢、炎症反应和癌症相关的信号通路。蛋白质互作网络和基因结构特征的分析结果显示, *CXCR4* (*C-X-C motif chemokine receptor 4*)、*PECAM1* (*platelet and endothelial cell adhesion molecule 1*)、*PLAU* (*urokinase-type plasminogen activator*)、*AGT* (*angiotensinogen*)、*AKT2* (*AKT serine/threonine kinase 2*)、*HSP70.2* (*heat shock cognate 70-kD protein, tandem duplicate 2*)、*LGALS3* (*galectin 3*)、*POSTN* (*periostin*)在调控网络中处于中心位置。此外, qRT-PCR验证结果和测序结果的趋势一致, 证明测序结果真实可靠。文中IMF和SCF转录组的差异分析结果提示, *AGT*、*CXCR4*、*HSP70.2*和*PLAU*基因在莱芜猪IMF沉积和脂代谢过程中发挥关键作用, 可作为调控IMF的候选基因。

关键词: 脂肪代谢; 肌肉脂肪(IMF); 皮下脂肪(SCF); 转录组测序; PCR验证

中图分类号: Q812, S828.2

文献标志码: A

文章编号: 1007-7847(2023)02-0179-10

Transcriptome Analysis of Intramuscular and Subcutaneous Fat of Laiwu Pig

FENG Hui, LIU Tianyi, SALSABEEL Yousuf, MIAO Xiangyang*

(Institute of Animal Sciences, Chinese Academy of Agricultural Sciences, Beijing 100193, China)

Abstract: In order to explore the hub genes for the difference of adipogenesis and lipid metabolism in different tissues of Laiwu pigs, Laiwu pigs with similar body weight at 180 days of age were used to identify the mRNA expression profiles of intramuscular fat (IMF) and subcutaneous fat (SCF). The functions of differentially expressed mRNAs were analyzed through Gene Ontology (GO) and Kyoto Encyclopedia of Genes and Genomes (KEGG). A protein-protein interaction (PPI) network of the top 300 mRNAs with a high average expression level was constructed, key regulatory mRNAs were screened, and sequence features and protein structures of the key mRNAs were analyzed. Meantime, the reliability of the sequencing data was verified by real-time fluorescence quantitative PCR (qRT-PCR) for 6 randomly selected mRNAs. A total of 1 665 differentially expressed mRNAs were identified from IMF and SCF mRNA expression profiles, of which 888 were up-regulated and 777 were down-regulated. The GO results showed that the differentially expressed mRNAs

收稿日期: 2021-11-10; 修回日期: 2022-01-10; 网络首发日期: 2022-05-20

基金项目: 转基因生物新品种培育科技重大专项(2009ZX08008-004, 2008ZX08008-003); 农业科技创新工程资助项目(ASTIP-IAS05); 中央级公益性科研院所基本科研业务费专项资金项目(Y2016JC22, Y2018PT68)

作者简介: 冯卉(1996—), 女, 河北廊坊人, 硕士, 主要从事动物遗传育种、分子生物学及生物信息学研究, E-mail: 1765516120@qq.com;

*通信作者: 苗向阳(1963—), 男, 山东莱州人, 博士, 研究员, 主要从事基因工程与功能基因组学研究, E-mail: miaoxy32@163.com。

were mainly involved in regulating signal pathways in biological process (BP); composing biological membranes in cellular component (CC); affecting the enzyme activity in the cell metabolism process in molecular function (MF). The KEGG enrichment results showed that the differentially expressed mRNAs were mainly involved in adipocyte production, lipid metabolism, inflammation and cancer-related signaling pathways. Through analysis of the PPI network, gene sequence and protein structure characteristics, it was found that *C-X-C motif chemokine receptor 4 (CXCR4)*, *platelet and endothelial cell adhesion molecule 1 (PECAM1)*, *urokinase-type plasminogen activator (PLAU)*, *angiotensinogen (AGT)*, *AKT serine/threonine kinase 2 (AKT2)*, *heat shock cognate 70-kD protein, tandem duplicate 2 (HSP70.2)*, *galectin 3 (LGALS3)*, and *periostin (POSTN)* were in the center of the regulatory network. The qRT-PCR verification results were consistent with the sequencing results, proving the reliability of sequencing results. By comparing the difference between IMF and SCF transcriptomes, it was found that *AGT*, *CXCR4*, *HSP70.2* and *PLAU* genes play critical roles in the lipid metabolism process of IMF deposition and can be used as candidate genes in IMF regulation.

Key words: fat metabolism; intramuscular fat (IMF); subcutaneous fat (SCF); transcriptome sequencing; PCR verification

(*Life Science Research*, 2023, 27(2): 179-188)

莱芜猪是我国优秀的地方猪种,其肉质细嫩,肌肉脂肪(intramuscular fat, IMF)和皮下脂肪(subcutaneous fat, SCF)沉积水平较高,与目前我国主要的商品猪种,例如大白猪、长白猪、杜洛克等,存在显著差异^[1-2]。最新研究发现,莱芜猪 IMF 的平均含量为 7%,最高能达到 18%^[3]。IMF 能够影响猪肉的营养价值和肉质风味,其含量高,则肉质细嫩、系水能力强、大理石花纹明显^[4]。SCF 是猪胴体评价指标,其沉积含量往往和瘦肉率成反比。IMF 和 SCF 都是白色脂肪,沉积部位不同,沉积含量也存在较大差异。有研究表明,白色脂肪在生物生长发育过程中首先在皮下沉积,当 SCF 沉积到一定程度后,白色脂肪开始在内脏、肌肉等其他部位沉积^[5]。所以,IMF 和 SCF 沉积具有协同性,即 IMF 沉积量越高,SCF 含量越高。随着人们对猪肉品质关注度的提高,在降低或不增加 SCF 含量的同时培育出高 IMF 含量的猪种也越来越成为畜牧研究者追求的育种目标。已有的研究证实,多种基因可在 IMF 沉积中发挥重要作用,例如 *FABP3 (fatty acid binding protein 3)*、*PDK4 (pyruvate dehydrogenase kinase 4)*、*FAM131B (family with sequence similarity 131 member B)*、*RIC8B (RIC8 guanine nucleotide exchange factor B)*、*PLEKHA5 (pleckstrin homology domain containing A5)*、*PARP6 [poly(ADP-ribose) polymerase family member 6]*和 *CBX7 (chromobox homolog 7)*等^[6-7]。在山羊 IMF 细胞中过表达 *PDK4*,能够极显著增加脂质积累和脂代谢相关基因 *FABP3*、*CD36*、*ACACA*

(*acetyl-CoA carboxylase alpha*)、*AGPAT6 (glycerol-3-phosphate acyltransferase 4)*和 *ADRP (perilipin 2)*的表达水平^[8]。Liu 等^[9]在体外培养猪 IMF 和 SCF 细胞并过表达 *CRTC3 (CREB regulated transcription coactivator 3)*,发现 IMF 细胞中的甘油磷脂代谢和 SCF 细胞中的 cAMP 信号通路发生显著改变。成纤维细胞生长因子(fibroblast growth factor, FGF)在脂质代谢中发挥重要作用,其中 *FGF21* 过表达能下调 IMF 细胞中 *PPARG (peroxisome proliferator-activated receptor gamma)*、*p2* 和 *SREBP1 (sterol regulatory element binding transcription factor 1)*的表达,抑制脂质积累^[10]; *FGF10* 过表达则能够促进山羊 IMF 细胞中脂质的累积^[11]。*CDC10 (cell division cycle 10)*过表达能够促进 IMF 和 3T3-L1 细胞增殖以及前体脂肪细胞分化^[12]。骆娜^[13]通过比较文昌鸡腹部脂肪和 IMF 发现, *GAPDH (glyceraldehyde-3-phosphate dehydrogenase)*、*LDHA (lactate dehydrogenase A)*、*GPX1 (glutathione peroxidase 1)*等基因促进 IMF 合成。Zhuang 等^[14]对杜洛克猪 IMF 进行了全基因组关联分析(genome-wide association study, GWAS),发现 *BDKRB2 (bradykinin receptor B2)*和 *ATG2B (autophagy-related 2B)*能够作为调节 IMF 沉积的候选基因。目前,应用 RNA-seq 技术探究影响 IMF 沉积的转录本也越来越受关注^[15-16]。本研究通过对比莱芜猪 IMF 和 SCF 组织的转录本差异,筛选出成脂分化和脂代谢相关基因,以期为进一步培育高瘦肉率和高肉品质的猪种提供新的思路和理论依据。

1 材料与方法

1.1 转录组深度测序

选取 3 头健康的体重相近的 180 日龄莱芜猪,取背最长肌处的 IMF 和 SCF 作为实验材料,分别记作 L_JN_1、L_JN_2、L_JN_3 和 L_PX_1、L_PX_2、L_PX_3。每个样品取 100 mg,应用 Trizol 法提取总 RNA。为验证 RNA 质量,采用凝胶电泳和 NanoDrop 检测总 RNA 的完整性、纯度和浓度。应用 Illumina HiSeq 2500 测序平台对总 RNA 进行深度测序,原始数据应用 NGS QC Toolkit (v2.3.3)^[17] 去除低质量片段,得到 clean reads。

1.2 差异表达 mRNA 的筛选

从 Ensemble 数据库 (<https://asia.ensembl.org/index.html>, 2020-06-07) 下载猪 (Sscrofa 10.2) 的参考基因组及转录本注释文件。采用 Tophat2^[18] 将 clean reads 对比到参考基因组,获取转录本的位置和序列特征信息。应用 cufflinks 程序对每个样品的比对结果进行概率模型重建,组装样本中的转录本,并对转录本表达量进行统计,结果以每千个碱基的转录每百万映射读取的片段数 (fragments per kilobase of exon per million fragments mapped, FPKM) 表示。应用 cuffcompare 程序对样品转录本和转录本注释文件进行逐一比较,获得样品转录本的注释信息。将鉴定得到的 mRNA 应用 R 语言中的 DESeq 包^[19] 进行差异 mRNA 表达分析,计算差异倍数 (fold change, FC), 当 $P \leq 0.05$ 且 $|\log_2(FC)| \geq 1$ 时,该 mRNA 在两个组织中的表达水平被认为存在显著差异。通过 pheatmap 包对各样本中显著差异表达的基因进行聚类分析。

1.3 差异表达 mRNA 的功能注释

得到差异表达转录本后,应用 R 语言中的 clusterProfiler 包^[20] 进行基因本体论 (Gene Ontology, GO) 功能注释与京都基因和基因组数据库 (Kyoto Encyclopedia of Genes and Genomes, KEGG) 富集

分析,结果以 $P \leq 0.05$ 为显著富集。

1.4 差异表达 mRNA 的蛋白质互作网络构建

按照平均表达量排序,取排名前 300 的 mRNA,应用 STRING 数据库 (<https://string-db.org/>, 2020-06-08) 对蛋白质-蛋白质相互作用 (protein-protein interaction, PPI) 关系进行预测,设置最低互作得分 (interaction score) 为 0.4 (中等置信度),其余参数选择默认值。将结果导入 Cytoscape 后,剔除不参与互作网络的单一蛋白质,得到最终的蛋白质-蛋白质互作网络图。

1.5 关键基因结构特征的分析

从 Gene 数据库 (<https://www.ncbi.nlm.nih.gov/gene>, 2020-06-08) 下载筛选得到的关键基因序列、编码序列 (coding sequence, CDS)、蛋白质序列等信息,使用 GSDS 2.0 在线分析网站 (<http://gsds.gao-lab.org/>, 2020-06-08) 将序列信息可视化处理。使用 MEME 在线分析网站 (<https://meme-suite.org/meme/doc/meme.html>, 2020-06-08) 对蛋白质序列进行模体 (motif) 预测, motif 结果可作为该蛋白质潜在的结合位点。同一蛋白质在细胞中表达的位置不同,其发挥的功能也存在差异^[21],为探究蛋白质表达位点和功能之间的关系,通过 UniProt 数据库 (<https://www.uniprot.org/>, 2020-06-08) 查询关键蛋白质的亚细胞定位。蛋白质的空间结构预测有助于更好地理解蛋白质功能,我们通过 SWISS-MODEL (<https://swissmodel.expasy.org/>, 2020-06-08) 预测关键基因的蛋白质三维结构。

1.6 qRT-PCR 验证

为进一步验证测序结果的可靠性,随机选取 6 个 mRNA 进行 qRT-PCR 验证,引物如表 1 所示。以 GAPDH 作为内参基因,使用 $2^{-\Delta\Delta Ct}$ 方法计算相对表达量。从 Gene 数据库中下载验证基因的 mRNA 序列,应用 NCBI 中的 BLAST 分析基因保守区域,获取引物序列后,由基普生物技术有限公司合成。

表 1 基因及引物信息

Table 1 The genes and their corresponding primer sequences

Gene	Sense (5'-3')	Antisense (5'-3')	Length/bp
MMP9	TGTTAAGGAGCACGGAGATCG	TGGCGTCCGGTGCATAGT	288
UBA7	ATGACCTGAAGTGGACCTGTTG	CGACCATCCTGCCGAGTAGA	158
PPARD	CGAGTTCGCCAAGAGCATCC	GCACGCCGTA CTGAGAAGG	77
CD180	CGAGGCTTCTGACTGTTGTGA	AGGTGCTGATTGCTGGTGTGTC	246
PODXL	ACTCCTCTGTTCTGTGACT	TGGCGTTATTGTAATCAGCATCTC	147
ELF4	GCTGGACGATGTTACAATGG	GAGCAAGACTTCAGTGGTGTGAC	139
GAPDH	TGAAGTCCGAGTGAACGGATT	CCATGTA CTGGAGGTCAATGAAGG	120

2 结果

2.1 原始数据分析结果

测序结果 clean reads 达到每个样本 10 G 以上, 且各样本 Q30>90%, 说明测序结果符合后续实验要求。将 clean reads 对比到参考基因组, 对比率均在 71%以上, 鉴定到各样本中 reads 的比对情况如表 2 所示。

2.2 差异表达 mRNA 筛选结果

以 $P \leq 0.05$ 且 $|\log_2(FC)| \geq 1$ 为条件, 在 IMF 和

SCF 中共筛选到 1 665 个差异表达的 mRNA, 其中 888 个表达上调, 777 个表达下调。对 IMF 和 SCF 中差异表达的 mRNA 进行聚类分析, 结果显示, IMF 样品 L_JN_1、L_JN_2、L_JN_3 和 SCF 样品 L_PX_1、L_PX_2、L_PX_3 分别聚类在一起, 且 mRNA 的上下调趋势一致, 说明实验样品和深度测序结果可靠。

2.3 差异表达 mRNA 的功能注释

对差异表达 mRNA 进行功能注释, 结果显示它们显著富集到 294 个 GO 条目, 其中包括 245

表 2 6 个样本对比参考基因组的结果

Table 2 The result of 6 samples after mapping to the reference genome

Reads	Sample					
	L_JN_1	L_JN_2	L_JN_3	L_PX_1	L_PX_2	L_PX_3
Total reads	88 890 352	89 083 366	91 659 768	89 189 416	91 416 676	88 944 438
Total mapped reads	65 333 853 (73.50%)	65 710 645 (73.76%)	67 630 486 (73.78%)	66 219 222 (74.25%)	65 157 231 (71.27%)	65 611 080 (73.77%)
Multiply mapped	11 406 632 (12.83%)	10 421 104 (11.70%)	11 270 084 (12.30%)	11 952 598 (13.40%)	9 223 144 (10.09%)	10 854 317 (12.20%)
Uniquely mapped	53 927 221 (60.67%)	55 289 541 (62.06%)	56 360 402 (61.49%)	54 266 624 (60.84%)	55 934 087 (61.19%)	54 756 763 (61.56%)
Reads mapped in proper pairs	27 209 176 (30.61%)	27 852 566 (31.27%)	28 451 724 (31.04%)	27 381 285 (30.70%)	28 138 575 (30.78%)	27 682 195 (31.12%)

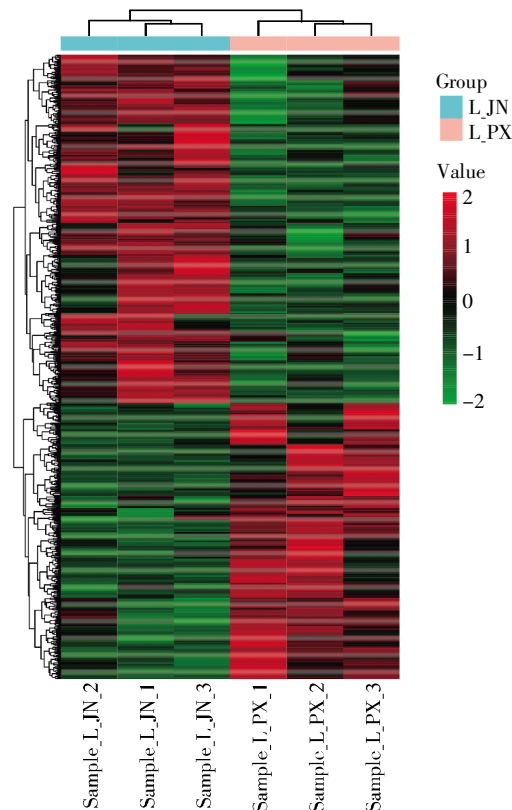


图 1 差异表达 mRNA 的聚类分析结果

“Value”表示丰度值行归一化之后的相对表达变化值。

Fig.1 Cluster analysis results of differentially expressed mRNAs

“Value” indicates the relative expression change value of the abundance after normalization.

个生物过程、24 个细胞组成和 25 个分子功能。选取各组分排名前 10 的 GO 条目进行展示,发现差异 mRNA 主要参与 JNK 级联的正调控、MyD88 依赖性 Toll 样受体信号通路、信号转导的正调控等生物过程; 主要涉及线粒体膜、膜面、膜微区等细胞组成; 参与的分子功能主要包括氧化还原酶活性、NAD(P)H 氧化还原酶活性、醌或类似化合物受体、NADH 脱氢酶(泛醌)活性等(图 2)。通路富集结果显示, 差异 mRNA 显著富集于 61 条信号通路, 排名前 30 的信号通路的展示结果见图 3。从图中可知, 差异 mRNA 显著富集于丝裂原活化蛋白激酶(mitogen-activated protein kinase, MAPK)信号通路、缺氧诱导因子 1 (hypoxia-inducible factor 1, HIF-1)信号通路、Wnt 信号通路、PI3K-Akt 信号通路、过氧化物酶体增殖物激活受体(peroxisome proliferator-activated receptor, PPAR)信号通路、哺乳动物雷帕霉素靶蛋白(mammalian target of rapamycin, mTOR)信号通路、Toll 样受体信号通路和胰岛素抵抗等。

2.4 蛋白质互作网络

图 4 的结果显示, *CXCR4*、*LGALS3*、*PLAU*、*AGT*、*AKT2*、*HSP70.2*、*PECAM1*、*POSTN* 等基因编码的蛋白质在互作网络中能够与更多的蛋白质发生相互作用, 处于调控网络的核心位置, 它们可作为关键基因用于后续分析。

2.5 关键基因的结构特征

经过蛋白质互作网络的筛选, 得到关键基因, 对关键基因进行序列特征和蛋白质特征分析, 结果见图 5。PECAM1 和 PLAU 蛋白质存在更多的 motif, 说明这些蛋白质可能存在更多潜在的结合位点。除 AKT2 外, 其他蛋白质在细胞内外广泛分布。结合表达量热图, 我们发现, *HSP70.2*、*AGT*、*CXCR4*、*PLAU* 在 IMF 组织表达上调且其蛋白质能预测到可信度较高的空间结构。

2.6 qRT-PCR 验证

随机选取 *MMP9* (*matrix metalloproteinase 9*)、*UBA7* (*ubiquitin like modifier activating enzyme 7*)、*PPARD*、*CD180*、*PODXL* (*podocalyxin like*)、*ELF4*

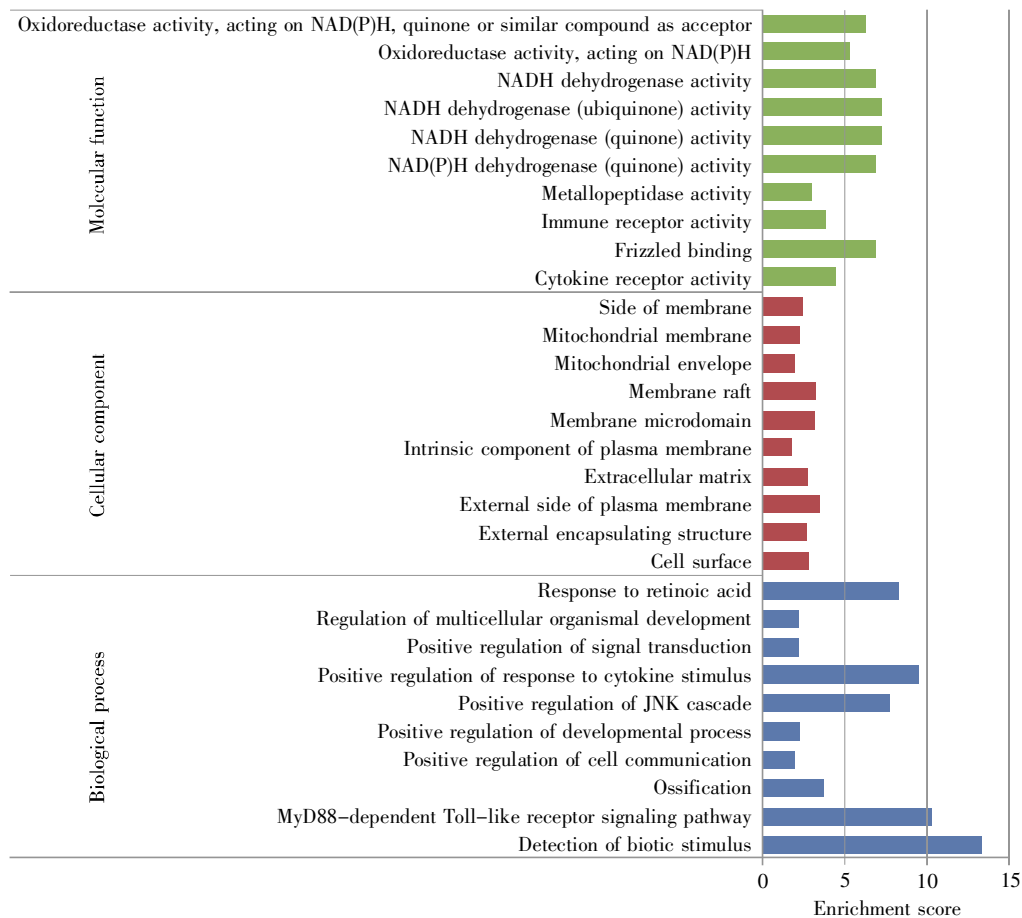


图 2 差异表达 mRNA 的 GO 功能注释(前 10 条)

Fig.2 GO enrichment analysis of differentially expressed mRNAs (top 10)

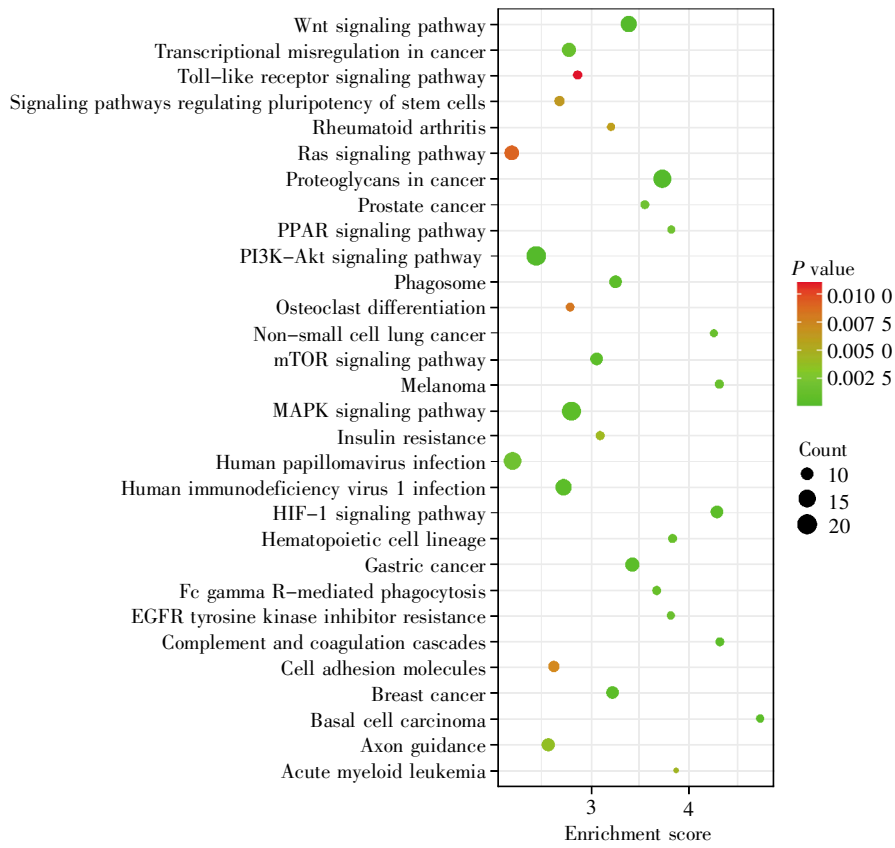


图 3 差异表达 mRNA 的 KEGG 信号通路富集(前 30 条)

Fig.3 KEGG pathway enrichment analysis of differentially expressed mRNAs (top 30)

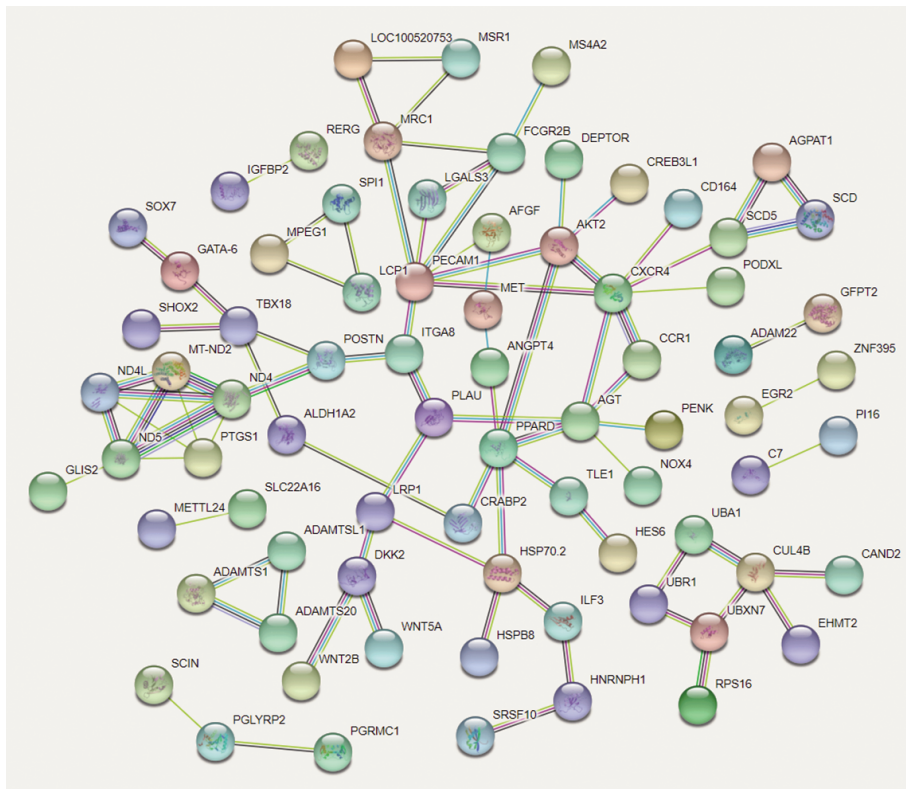


图 4 前 300 mRNA 的蛋白质-蛋白质互作网络

Fig.4 PPI network of the top 300 mRNAs

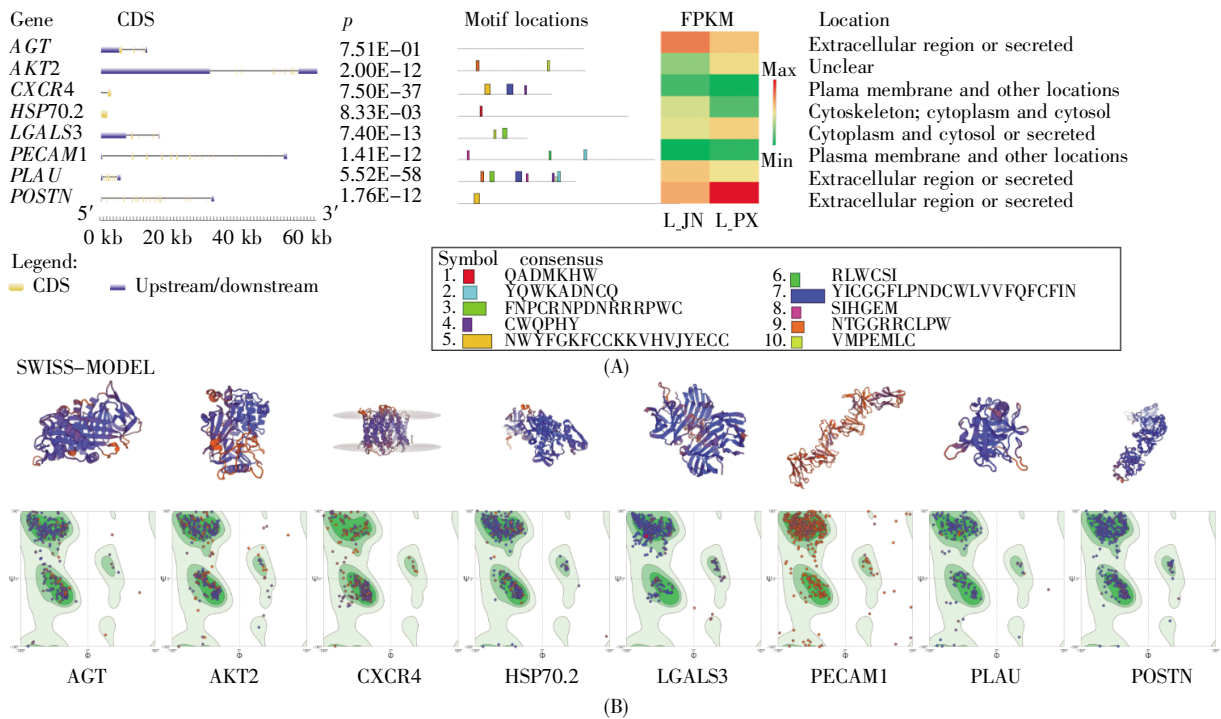


图 5 关键基因序列结构(A)和蛋白质结构(B)分析

p 值表示该基因对应 mRNA 的模体预测置信度。

Fig.5 Sequence structure (A) and protein structure (B) analysis of the key genes

p value indicates the predictive confidence of the motif of the mRNA corresponding to the gene.

(*E74 like ETS transcription factor 4*)共 6 个 mRNA 进行 qRT-PCR 验证。结果如图 6 所示,其在两组样品中的表达趋势与测序结果的趋势一致,证明测序结果准确。

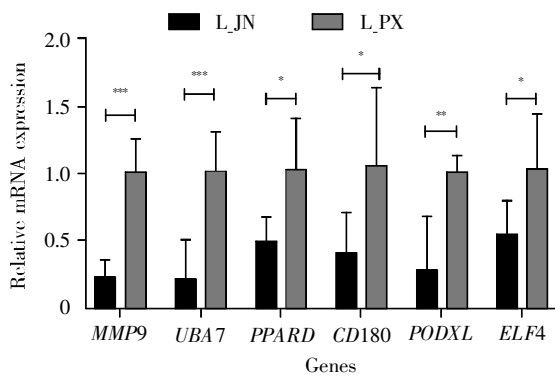


图 6 6 个差异表达 mRNA 的 qRT-PCR 验证结果

数据为平均值±标准差, **P*≤0.05, ***P*≤0.01, ****P*≤0.001。

Fig.6 qRT-PCR verification results of 6 mRNAs

The data is mean ± standard deviation, **P*≤0.05, ***P*≤0.01, ****P*≤0.001.

3 讨论

本研究通过对 IMF 和 SCF 的转录本进行深度测序,筛选出在两个组织中差异表达的 mRNA

共 1 665 个。对差异表达的 mRNA 进行功能注释分析,结果显示,它们显著富集在脂肪细胞增殖、分化和脂质代谢相关的 GO 条目和 KEGG 信号通路(图 2 和图 3)。

PPAR 信号通路是间充质干细胞向前体脂肪细胞增殖、分化和脂质代谢等过程的关键调节通路,PPARG 是该通路中最关键的转录调控因子^[22]。当 Wnt 信号通路激活时,β-catenin 和 TCF/LEF (transcription factor/lymphoid enhancer-binding factor)形成复合蛋白质进入前体脂肪细胞核,促进 *CBP* (*CREB binding protein*)、*PYGO* (*pygopus*)、*BCL-9*、*p300* 等基因的表达^[23]。这些基因能够促进前体脂肪细胞增殖、分化,或者促进脂肪细胞释放脂肪因子,从而促进脂肪细胞成熟。其中, *CBP* 作为转录辅激活因子与活化的 CREB (cAMP responsive element binding protein 1)结合,激活 PPAR 信号通路;同时, *CBP* 也能通过 LXR-C/EBPs-SREBPs 介导的调控轴在脂代谢中发挥重要作用^[24]。PI3K-Akt 信号通路受胰岛素调控,其通过激活 p-AS160 和 GLUT4 (glucose transporter 4),促进葡萄糖转运和代谢,进而减缓胰岛素抵抗^[25]。PI3K-Akt 信号通路在 C2C12 细胞诱导分化为脂肪细胞的早期被激活,促进脂质积累^[26]。此外,PI3K-Akt 信号通

路还能够激活 mTOR 信号通路, mTOR 复合物则通过激活 *SRPK2* (*SRSF protein kinase 2*) 基因促进脂质生成^[27]。MAPK 信号通路主要通过胞外信号调节激酶(extracellular signal-regulated kinase, ERK)、p38 MAPK 和 c-Jun 氨基端蛋白激酶(c-Jun N-terminal protein kinase, JNK) 3 条途径, 参与脂肪细胞的分化调节^[28]。其中, JNK 使胰岛素受体磷酸化, 抑制成脂分化过程, 而 ERK 和 p38 MAPK 的调控机制较为复杂, 既能促进也能抑制成脂分化过程^[29]。在本实验中, IMF 和 SCF 差异表达的 mRNA 显著富集于 PPAR、Wnt、PI3K-Akt、mTOR、MAPK 信号通路和胰岛素抵抗, 说明差异表达 mRNA 主要参与脂肪细胞的增殖、分化和脂质代谢调节。

通过蛋白质互作网络进一步筛选影响不同部位脂肪沉积的差异基因, 结果显示 *CXCR4*、*LGALS3*、*PLAU*、*AGT*、*AKT2*、*HSP70.2*、*PECAM1*、*POSTN* 等编码的蛋白质能够与更多的蛋白质发生相互作用(图 4), 提示它们可作为关键基因用于后续分析。关键基因的序列、蛋白质特征、亚细胞定位等分析结果显示, *AGT*、*CXCR4*、*HSP70.2*、*PLAU* 在 IMF 中有较高表达, 对应蛋白质具有稳定的空间结构, 且在细胞中分布广泛(图 4), 可作为 IMF 调控的候选基因。

脂肪组织是血管紧张素原(angiotensinogen, AGT)的重要来源, 但在目前的动物模型研究中, 不同脂肪组织之间的 AGT 表达水平和功能差异较大。有研究发现, AGT 及其产物血管紧张素 II (angiotensin II, Ang II), 能够影响前体脂肪细胞和脂肪细胞的分化及代谢^[30]; 敲除特定脂肪组织 AGT 的小鼠表现出脂肪炎症减少, 脂肪细胞的葡萄糖代谢增加^[31]。相关研究报道, 在体外培养的 3T3-L1 细胞中沉默 *AGT* 基因, 可减少 Ang II 的含量, 导致细胞中脂质增加^[32]; Ang II 在前体脂肪细胞中促进 MAPK/ERK12 和 PPARC 磷酸化, 降低前体脂肪细胞向脂肪细胞的分化^[33]。热休克蛋白 $\beta 1$ [*heat shock protein family B (small) member 1*, *HSPB1*] 是已被证实的 IMF 调控基因, 其存在 *AGT* 结合位点, 当 *AGT* 过表达时, *HSPB1* 表达量降低, 从而影响 IMF 含量^[34]。本研究中 *AGT* 在 IMF 的表达水平显著高于其他关键基因, 推测其可能是限制 IMF 沉积的主要候选基因。*CXCR4* 参与多种细胞的发育过程, 包括造血干细胞、淋巴细胞和 NK 细胞等, 能够促进肿瘤的发生^[35]。刺激 3T3-L1 细胞 PPAR 信号通路表达后, 研究人员发现 *CXCR4* 表达量显著增加^[36], 说明 *CXCR4* 可能参与脂肪细

胞增殖、分化和脂质代谢。脂肪细胞 *CXCR4* 能够调控棕色脂肪标志基因 *UCP1* (*uncoupling protein 1*) 介导的能量消耗, 维持脂肪组织平衡^[37]。有研究报道, 小鼠出生后 *CXCR4* 在后肢肌肉的表达量一直维持在较低水平; 当在体外增殖培养 C2C12 时, *CXCR4* 表达量升高, 在细胞进入分化阶段时, *CXCR4* 表达水平保持不变^[38]。在本研究中, *CXCR4* 在 IMF 中的表达量增加, 与前人研究结果^[35-38]一致, 说明 *CXCR4* 是一种潜在的 IMF 细胞标志性基因, 在猪出生后对 *CXCR4* 的转录后进行调控, 有可能在不影响肌肉质量的情况下增加 IMF 含量。在热应激、炎症、辐射、缺氧等不良刺激下, 热休克蛋白(heat shock protein, HSP)表达增加, 从而增加细胞耐受性, 缓解细胞损伤, 保护机体使其减少应激^[34]。*HSP70* 是慢性糖尿病(T2DM)的标志性基因, 抑制 *HSP70* 的表达可以激活 JNK 信号通路、诱发炎症、减少线粒体、抑制线粒体脂肪酸氧化, 导致胰岛素抵抗^[39]。研究发现, *HSP70* 在细胞内外的表达功能存在差异, 细胞内 *HSP70* (i *HSP70*) 抑制 NF- κ B 信号通路激活, 降低炎症和胰岛素抵抗; 细胞外 *HSP70* (e *HSP70*) 激活一系列促进炎症的信号通路^[21, 40]。*HSP70* 对肌原分化有促进作用, 在体外培养的 C2C12 细胞中过表达 *HSP70* 能够促进肌细胞融合^[41]; 在降低或敲除 *HSP70* 的实验中, 肌细胞分化受到抑制^[42]。在本研究中, *HSP70.2* 的表达在 IMF 中显著上调, 而 *HSP70.2* 基因多态性与人类肥胖症显著相关^[43], 推测其可能通过促进肌原细胞增殖、分化和细胞融合, 降低脂肪细胞炎症和胰岛素抵抗, 从而限制 IMF 含量。尿素酶型纤溶酶原激活物(urokinase-type plasminogen activator, *PLAU*) 在纤维化、癌症转移、动脉粥样硬化和阿尔茨海默病中起着重要的生理和病理作用^[44-45]。有研究表明, *PLAU* 能够调节人类胆固醇生物合成^[46]。敲除 *PLAU* 基因的肥胖小鼠比野生型肥胖小鼠表现出更好的葡萄糖代谢, 同时能够通过磷酸化肝细胞生长因子抑制炎症^[47]。本研究中, *PLAU* 在 IMF 和 SCF 中均有较高水平的表达, 且参与脂肪细胞的能量代谢, 也可作为影响不同部位脂肪代谢的候选基因。综上可知, *AGT*、*CXCR4*、*HSP70.2* 和 *PLAU* 可作为 IMF 调控研究的候选基因, 但作用机制还有待进一步挖掘。

4 总结

IMF 和 SCF 均属于白色脂肪, 由于沉积部位

不同, 脂肪含量存在较大差异。为探究产生差异的关键基因, 本实验对莱芜猪 IMF 和 SCF 进行了转录组深度测序及生物信息学分析, 结果显示: 两种脂肪组织中的 1 665 个差异 mRNA 显著富集在与脂肪细胞增殖、分化和代谢相关的 GO 条目和 KEGG 信号通路; 其中, *AGT*、*CXCR4*、*HSP70.2* 和 *PLAU* 可能是调节 IMF 沉积的关键基因。

参考文献(References):

- [1] HUANG W L, ZHANG X X, LI A, *et al.* Genome-wide analysis of mRNAs and lncRNAs of intramuscular fat related to lipid metabolism in two pig breeds[J]. *Cellular Physiology and Biochemistry*, 2018, 50(6): 2406–2422.
- [2] LI A, HUANG W L, ZHANG X X, *et al.* Identification and characterization of circRNAs of two pig breeds as a new biomarker in metabolism-related diseases[J]. *Cellular Physiology and Biochemistry*, 2018, 47(6): 2458–2470.
- [3] 任一帆, 赵雪艳, 王彦平, 等. 莱芜猪与杜长大肉质性状比较与分析[J]. 养猪(REN Yifan, ZHAO Xueyan, WANG Yaping, *et al.* Comparison of carcass traits and meat quality between Laiwu pig and Duroc×Landrace×Yorkshire pigs[J]. *Swine Production*), 2021(5): 45–48.
- [4] 宿甲子, 孙肖明, 孟宪梅. 肌肉脂肪对猪肉品质的影响及研究进展[J]. 畜牧兽医科技信息(SU Jiazi, SUN Xiaoming, MENG Xianmei. Effect of intramuscular fat on pork quality and its research progress[J]. *Chinese Journal of Animal Husbandry and Veterinary Medicine*), 2020(10): 19–20.
- [5] CRISTANCHO A G, LAZAR M A. Forming functional fat: a growing understanding of adipocyte differentiation[J]. *Nature Reviews Molecular Cell Biology*, 2011, 12(11): 722–734.
- [6] 刘娟, 王舒, 左周, 等. 结合 WGCNA 鉴定与猪肌纤维和肌肉脂肪相关的中枢基因[J]. 山西农业大学学报(自然科学版)(LIU Juan, WANG Shu, ZUO Zhou, *et al.* Identification of hub genes associated with porcine muscle fibers and intramuscular fat by WGCNA[J]. *Journal of Shanxi Agricultural University (Natural Science Edition)*), 2021, 41(4): 109–118.
- [7] 苗海明, 高爱武, 杨金丽, 等. 动物肌肉脂肪沉积对肉嫩度影响的研究进展[J]. 中国农学通报(MIAO Haiming, GAO Aiwu, YANG Jinli, *et al.* The advances of the effects of intramuscular fat deposition on the meat tenderness[J]. *Chinese Agricultural Science Bulletin*), 2012, 28(11): 51–54.
- [8] 张浩, 张亚楠, 李鑫, 等. PDK4 对山羊肌肉脂肪细胞脂代谢的影响[J]. 生物技术通报(ZHANG Hao, ZHANG Yanan, LI Xin, *et al.* Effect of PDK4 on the lipid metabolism of goat intramuscular adipocytes[J]. *Biotechnology Bulletin*), 2021, 37(12): 151–159.
- [9] LIU J Q, WANG L Y, CHEN W T, *et al.* CRTC3 regulates the lipid metabolism and adipogenic differentiation of porcine intramuscular and subcutaneous adipocytes by activating the calcium pathway[J]. *Journal of Agricultural and Food Chemistry*, 2021, 69(25): 7243–7255.
- [10] XU Q, LIN S, LI Q, *et al.* Fibroblast growth factor 21 regulates lipid accumulation and adipogenesis in goat intramuscular adipocyte[J]. *Animal Biotechnology*, 2021, 32(3): 318–326.
- [11] XU Q, LIN S, WANG Y, *et al.* Fibroblast growth factor 10 (FGF10) promotes the adipogenesis of intramuscular preadipocytes in goat[J]. *Molecular Biology Reports*, 2018, 45(6): 1881–1888.
- [12] 程子轩. 牛 *CDC10* 基因多态性分析及调控肌肉脂肪细胞增殖与分化的机制[D]. 呼和浩特: 内蒙古大学(CHENG Zixuan. Polymorphism Analysis of Bovine *CDC10* Gene and Its Mechanism of Regulating Proliferation and Differentiation of Intramuscular Preadipocytes[D]. Hohhot: Inner Mongolia University), 2021.
- [13] 骆娜. 鸡肌肉脂肪和腹腔脂肪差异沉积的分子机理解析[D]. 北京: 中国农业科学院(LUO Na. Molecular Mechanism of Differential Deposition of Intramuscular Fat and Abdominal Fat in Chi-
- cken[D]. Beijing: Chinese Academy of Agricultural Sciences), 2021.
- [14] ZHUANG Z, DING R, QIU Y, *et al.* A large-scale genome-wide association analysis reveals QTL and candidate genes for intramuscular fat content in Duroc pigs[J]. *Animal Genetics*, 2021, 52(4): 518–522.
- [15] 黄万龙, 张秀秀, 李媛, 等. 利用 RNA-seq 技术筛选大白猪皮下和肌肉脂肪组织差异表达基因[J]. 遗传(HUANG Wanlong, ZHANG Xiuxiu, LI Ai, *et al.* Identification of differentially expressed genes between subcutaneous and intramuscular adipose tissue of Large White pig using RNA-seq[J]. *Hereditas*), 2017, 39(6): 501–511.
- [16] 李媛, 张秀秀, 黄万龙, 等. 大白猪和莱芜猪肌肉脂肪组织 circRNAs 的鉴定与分析[J]. 畜牧兽医学报(LI Ai, ZHANG Xiuxiu, HUANG Wanlong, *et al.* Identification and analysis of circRNAs in intramuscular adipose tissues between large white and Laiwu pigs[J]. *Acta Veterinaria et Zootechnica Sinica*), 2018, 49(7): 1343–1353.
- [17] HANSEN K D, BRENNER S E, DUDOIT S. Biases in illumina transcriptome sequencing caused by random hexamer priming[J]. *Nucleic Acids Research*, 2010, 38(12): e131.
- [18] KIM D, PERTEA G, TRAPNELL C, *et al.* TopHat2: accurate alignment of transcriptomes in the presence of insertions, deletions and gene fusions[J]. *Genome Biology*, 2013, 14(4): R36.
- [19] ANDERS S, HUBER W. Differential expression analysis for sequence count data[J]. *Genome Biology*, 2010, 11(10): R106.
- [20] YU G C, WANG L G, HAN Y Y, *et al.* clusterProfiler: an R package for comparing biological themes among gene clusters[J]. *OMICS*, 2012, 16(5): 284–287.
- [21] KRAUSE M, HECK T G, BITTENCOURT A, *et al.* The chaperone balance hypothesis: the importance of the extracellular to intracellular HSP70 ratio to inflammation-driven type 2 diabetes, the effect of exercise, and the implications for clinical management[J]. *Mediators of Inflammation*, 2015, 2015: 249205.
- [22] OKUNO A, TAMEMOTO H, TOBE K, *et al.* Troglitazone increases the number of small adipocytes without the change of white adipose tissue mass in obese Zucker rats[J]. *The Journal of Clinical Investigation*, 1998, 101(6): 1354–1361.
- [23] CHEN N, WANG J Q. Wnt/β-catenin signaling and obesity[J]. *Frontiers in Physiology*, 2018, 9: 792.
- [24] 苗春木, 赵蕾, 龚建平, 等. 转录辅激活因子 CBP 在脂代谢中的作用[J]. 医学分子生物学杂志(MIAO Chunmu, ZHAO Lei, GONG Jianping, *et al.* Function of transcription coactivator CBP in lipid metabolism[J]. *Journal of Medical Molecular Biology*), 2006, 3(5): 387–390, 400.
- [25] WANG J K, HE Y T, YU D Q, *et al.* Perilla oil regulates intestinal microbiota and alleviates insulin resistance through the PI3K/AKT signaling pathway in type-2 diabetic KKAy mice[J]. *Food and Chemical Toxicology*, 2020, 135: 110965.
- [26] 齐仁立, 黄晓凤, 吴泳江, 等. PI3K/Akt 在 C2C12 肌细胞脂肪分化中的作用[J]. 生物化学与生物物理进展(QI Renli, HUANG Xiaofeng, WU Yongjiang, *et al.* Role of PI3K/Akt in the adipogenic trans-differentiation of C2C12 myoblasts[J]. *Progress in Biochemistry and Biophysics*), 2017, 44(3): 224–231.
- [27] CHEN J X, CHEN J D, HUANG J X, *et al.* HIF-2α upregulation mediated by hypoxia promotes NAFLD-HCC progression by activating lipid synthesis via the PI3K-AKT-mTOR pathway[J]. *Aging*, 2019, 11(23): 10839–10860.
- [28] 周华, 蔡国平. MAPK 信号通路脂肪细胞分化[J]. 生命的化学(ZHOU Hua, CAI Guoping. MAPK signal pathway and adipocyte differentiation[J]. *Chemistry of Life*), 2006, 26(6): 505–507.
- [29] 苏健, 苏恒. 脂肪细胞分化过程中 MAPK 信号通路的调控机制[J]. 生命的化学(SU Jian, SU Heng. The regulation mechanism of MAPK signaling pathway in adipocyte differentiation[J]. *Chemistry of Life*), 2016, 36(2): 252–256.
- [30] AILHAUD G, TEBOUL M, MASSIERA F. Angiotensinogen, adipocyte differentiation and fat mass enlargement[J]. *Current Opinion in Clinical Nutrition and Metabolic Care*, 2002, 5(4): 385–389.
- [31] LEMIEUX M J, RAMALINGAM L, MYNATT R L, *et al.* Inactivation of adipose angiotensinogen reduces adipose tissue macrophages and increases metabolic activity[J]. *Obesity*, 2016, 24(2): 359–367.

- [32] CARROLL W X, KALUPAHANA N S, BOOKER S L, *et al.* Angiotensinogen gene silencing reduces markers of lipid accumulation and inflammation in cultured adipocytes[J]. *Frontiers in Endocrinology*, 2013, 4: 10.
- [33] FUENTES P, ACUÑA M J, CIFUENTES M, *et al.* The anti-adipogenic effect of angiotensin II on human preadipose cells involves ERK_{1/2} activation and PPAR γ phosphorylation[J]. *Journal of Endocrinology*, 2010, 206(1): 75–83.
- [34] KIM N K, LIM D, LEE S H, *et al.* Heat shock protein B1 and its regulator genes are negatively correlated with intramuscular fat content in the longissimus thoracis muscle of Hanwoo (Korean cattle) steers[J]. *Journal of Agricultural and Food Chemistry*, 2011, 59(10): 5657–5664.
- [35] POZZOBON T, GOLDONI G, VIOLA A, *et al.* CXCR4 signaling in health and disease[J]. *Immunology Letters*, 2016, 177: 6–15.
- [36] MA W S, LU S M, SUN T, *et al.* Twist 1 regulates the expression of PPAR γ during hormone-induced 3T3-L1 preadipocyte differentiation: a possible role in obesity and associated diseases[J]. *Lipids in Health and Disease*, 2014, 13: 132.
- [37] YAO L B, HEUSER-BAKER J, HERLEA-PANA O, *et al.* Deficiency in adipocyte chemokine receptor CXCR4 exacerbates obesity and compromises thermoregulatory responses of brown adipose tissue in a mouse model of diet-induced obesity[J]. *FASEB Journal*, 2014, 28(10): 4534–4550.
- [38] HUNGER C, ÖDEMIS V, ENGELE J. Expression and function of the SDF-1 chemokine receptors CXCR4 and CXCR7 during mouse limb muscle development and regeneration[J]. *Experimental Cell Research*, 2012, 318(17): 2178–2190.
- [39] MULYANI W R W, SANJIWANI M I D, SANDRA, *et al.* Chaperone-based therapeutic target innovation: heat shock protein 70 (HSP70) for type 2 diabetes mellitus[J]. *Diabetes, Metabolic Syndrome and Obesity: Targets and Therapy*, 2020, 13: 559–568.
- [40] ALEMI H, KHALOO P, RABIZADEH S, *et al.* Association of extracellular heat shock protein 70 and insulin resistance in type 2 diabetes; independent of obesity and C-reactive protein[J]. *Cell Stress & Chaperones*, 2019, 24(1): 69–75.
- [41] THAKUR S S, SWIDERSKI K, CHHEN V L, *et al.* HSP70 drives myoblast fusion during C2C12 myogenic differentiation[J]. *Biology Open*, 2020, 9(7): bio053918.
- [42] FAN W, GAO X K, RAO X S, *et al.* Hsp70 interacts with mitogen-activated protein kinase (MAPK)-activated protein kinase 2 to regulate p38MAPK stability and myoblast differentiation during skeletal muscle regeneration[J]. *Molecular and Cellular Biology*, 2018, 38(24): e00211–18.
- [43] MARDAN-NIK M, PASDAR A, JAMIALAHMADI K, *et al.* Association of heat shock protein70–2 (HSP70–2) gene polymorphism with obesity[J]. *Annals of Human Biology*, 2016, 43(6): 542–546.
- [44] PESARESI M, BATELLI S, PRATO F, *et al.* The urokinase-type plasminogen activator polymorphism *PLAU*_1 is a risk factor for *APOE*- ϵ 4 non-carriers in the Italian Alzheimer's disease population and does not affect the plasma *A β* (1–42) level[J]. *Neurobiology of Disease*, 2007, 25(3): 609–613.
- [45] AI C, ZHANG J X, LIAN S Y, *et al.* FOXM1 functions collaboratively with *PLAU* to promote gastric cancer progression[J]. *Journal of Cancer*, 2020, 11(4): 788–794.
- [46] TAMURA T, MORITA E, KAWAI S, *et al.* Significant association of *urokinase plasminogen activator* Pro141Leu with serum lipid profiles in a Japanese population[J]. *Gene*, 2013, 524(2): 363–367.
- [47] COUDRIET G M, STOOPE J, ORR A V, *et al.* A noncanonical role for plasminogen activator inhibitor type 1 in obesity-induced diabetes[J]. *The American Journal of Pathology*, 2019, 189(7): 1413–1422.

(上接第 154 页)

- [52] SEWALD X, GEBERT-VOGL B, PRASSL S, *et al.* Integrin subunit CD18 is the T-lymphocyte receptor for the *Helicobacter pylori* vacuolating cytotoxin[J]. *Cell Host & Microbe*, 2008, 3(1): 20–29.
- [53] GEBERT B, FISCHER W, WEISS E, *et al.* *Helicobacter pylori* vacuolating cytotoxin inhibits T lymphocyte activation[J]. *Science*, 2003, 301(5636): 1099–1102.
- [54] AKASHI T, ISOMOTO H, MATSUSHIMA K, *et al.* A novel method for rapid detection of a *Helicobacter pylori* infection using a γ -glutamyltranspeptidase-activatable fluorescent probe[J]. *Scientific Reports*, 2019, 9: 9467.
- [55] WÜSTNER S, ANDERL F, WANISCH A, *et al.* *Helicobacter pylori* γ -glutamyl transferase contributes to colonization and differential recruitment of T cells during persistence[J]. *Scientific Reports*, 2017, 7: 13636.
- [56] RIMBARA E, MORI S, KIM H, *et al.* Role of γ -glutamyltranspeptidase in the pathogenesis of *Helicobacter pylori* infection[J]. *Microbiology and Immunology*, 2013, 57(10): 665–673.
- [57] OWYANG S Y, ZHANG M, EL-ZAATARI M, *et al.* Dendritic cell-derived TGF- β mediates the induction of mucosal regulatory T-cell response to *Helicobacter* infection essential for maintenance of immune tolerance in mice[J]. *Helicobacter*, 2020, 25(6): e12763.
- [58] QARIA M A, QUMAR S, SEPE L P, *et al.* Cholesterol glucosylation-based survival strategy in *Helicobacter pylori*[J]. *Helicobacter*, 2021, 26(2): e12777.
- [59] NAGATA M, TOYONAGA K, ISHIKAWA E, *et al.* *Helicobacter pylori* metabolites exacerbate gastritis through C-type lectin receptors[J]. *Journal of Experimental Medicine*, 2021, 218(1): e20200815.
- [60] WUNDER C, CHURIN Y, WINAU F, *et al.* Cholesterol glucosylation promotes immune evasion by *Helicobacter pylori*[J]. *Nature Medicine*, 2006, 12(9): 1030–1038.
- [61] HUANG Z, LONDON E. Cholesterol lipids and cholesterol-containing lipid rafts in bacteria[J]. *Chemistry and Physics of Lipids*, 2016, 199: 11–16.
- [62] QARIA M A, KUMAR N, HUSSAIN A, *et al.* Roles of cholesteryl- α -glucoside transferase and cholesteryl glucosides in maintenance of *Helicobacter pylori* morphology, cell wall integrity, and resistance to antibiotics[J]. *mBio*, 2018, 9(6): e01523–18.
- [63] DU S Y, WANG H J, CHENG H H, *et al.* Cholesterol glucosylation by *Helicobacter pylori* delays internalization and arrests phagosome maturation in macrophages[J]. *Journal of Microbiology, Immunology, and Infection*, 2016, 49(5): 636–645.
- [64] LAI C H, HUANG J C, CHENG H H, *et al.* *Helicobacter pylori* cholesterol glucosylation modulates autophagy for increasing intracellular survival in macrophages[J]. *Cellular Microbiology*, 2018, 20(12): e12947.
- [65] MOREY P, PFANNKUCH L, PANG E, *et al.* *Helicobacter pylori* depletes cholesterol in gastric glands to prevent interferon gamma signaling and escape the inflammatory response[J]. *Gastroenterology*, 2018, 154(5): 1391–1404.e9.
- [66] KUO C J, CHEN C Y, LO H R, *et al.* *Helicobacter pylori* induces IL-33 production and recruits ST-2 to lipid rafts to exacerbate inflammation[J]. *Cells*, 2019, 8(10): 1290.
- [67] HUTTON M L, KAPARAKIS-LIASKOS M, TURNER L, *et al.* *Helicobacter pylori* exploits cholesterol-rich microdomains for induction of NF- κ B-dependent responses and peptidoglycan delivery in epithelial cells[J]. *Infection and Immunity*, 2010, 78(11): 4523–4531.
- [68] 赵翠, 赵文莹, 赵福广. 幽门螺旋杆菌 *lpp20-cagA* 融合基因在乳酸球菌中的表达及免疫原性研究[J]. *中国预防兽医学报* (ZHAO Cui, ZHAO Wenxuan, ZHAO Fuguang. Expression and immunogenicity analysis of *Helicobacter pylori lpp20-cagA* fusion gene in *Lactococcus lactis*[J]. *Chinese Journal of Preventive Veterinary Medicine*), 2019, 41(6): 627–631.
- [69] HU C P, LIU W, XU N Y, *et al.* Perivascular lymphocyte clusters induced by gastric subserous layer vaccination mediate optimal immunity against *Helicobacter* through facilitating immune cell infiltration and local antibody response[J]. *Journal of Immunology Research*, 2020, 2020: 1480281.
- [70] MALEKI KAKELAR H, BARZEGARI A, DEGHANI J, *et al.* Pathogenicity of *Helicobacter pylori* in cancer development and impacts of vaccination[J]. *Gastric Cancer*, 2019, 22(1): 23–36.